Last century warming over the Canadian Atlantic shelves linked to weak Atlantic Meridional Overturning Circulation

Benoit Thibodeau[1,1], Christelle Not[1,1], Jiang Zhu[2,2], Andreas Schmittner[3,3,3,3], David Noone[3,3,3,3], Clay Tabor[4,4], Jiaxu Zhang[5,5,5,5], and Zhengyu Liu[6,6]

[1]The University of Hong Kong
[2]University of Michigan
[3]Oregon State University
[4]University of Connecticut
[5]Los Alamos National Laboratory
[6]The Ohio State University

August 16, 2018

Abstract

The Atlantic meridional overturning circulation (AMOC) is a key component of the global climate system. Many models predict a weakening or even a collapse of the AMOC under future climate change. Recent studies suggested a 20th century weakening of the AMOC of unprecedented amplitude (? 15%) over the last millennium. Here, we present δ18O of benthic foraminifera in a sediment core from the Laurentian Channel and demonstrate that the δ18O trend is linked to the strength of the AMOC. In this 100-year record, the AMOC signal decrease steadily to reach its minimum value in the late 1970's. The weakest AMOC signal is constant until 2000. We present a longer δ18O record of 1,500 years and highlight the uniqueness of these high δ18O values over that period. Moreover, the long record is also characterized by statistically heavier δ18O during the Little Ice age suggesting a relatively weak AMOC.

Preprint of:

Last century warming over the Canadian Atlantic shelves linked to weak Atlantic Meridional Overturning Circulation

Authors

B. Thibodeau[1,2]†*, C. Not[1,2]†, J. Zhu[3], A. Schmittner[4], D. Noone[4], C. Tabor[5], J. Zhang[6], Z. Liu[7]

Affiliations

[1]Department of Earth Sciences, The University of Hong Kong, Hong Kong SAR

[2]The Swire Institute of Marine Science, The University of Hong Kong, Hong Kong SAR

[3]Department of Earth and Environmental Sciences, University of Michigan, United-States of America

[4]College of Earth, Ocean, and Atmospheric Sciences, Oregon State University, United-States of America

[5]Center for Integrative Geosciences, University of Connecticut, United-States of America

[6]CCS-2 and CNLS, Los Alamos National Laboratory, Los Alamos, New Mexico, United-States of America

[7]Atmospheric Science Program, Department of Geography, The Ohio State University, United-States of America

*Correspondence to: bthib@hku.hk

† Equal contribution

Abstract

The Atlantic meridional overturning circulation (AMOC) is a key component of the global climate system. Recent studies suggested a 20th-century weakening of the AMOC of unprecedented amplitude (~ 15%) over the last millennium. Here, we present a record of $\delta^{18}O$ in benthic foraminifera from sediment cores retrieved from the Laurentian Channel and demonstrate that the $\delta^{18}O$ trend is linked to the strength of the AMOC. In this 100-year record, the AMOC signal decreased steadily to reach its minimum value in the late 1970's, where the weakest AMOC signal then remains constant until 2000. We also present a longer $\delta^{18}O$ record of 1,500 years and highlight the uniqueness of the last century $\delta^{18}O$ trend. Moreover, the Little Ice Age period is characterized by statistically heavier $\delta^{18}O$, suggesting a relatively weak AMOC. Implications for understanding the mechanisms driving the intensity of AMOC under global warming and high-latitude freshwater input are discussed.

1. Introduction

The Atlantic meridional overturning circulation (AMOC) encompasses the advection of warm and saline waters in the upper ocean to the northern parts of the Atlantic, where it cools, becomes denser and sinks, ultimately creating North Atlantic deep water. Both observational and modeling studies have suggested that the strength of this oceanic circulation cell is not constant through time (Bohm et al., 2015; Rahmstorf et al., 2015), and that these changes drive many other climatic events across wide ranges of spatial and temporal scales (Delworth et al., 2008). Weakening of the AMOC as a response to warming and/or high latitude freshwater release is a common feature of many climate models (Bakker et al., 2016; Jungclaus et al., 2006; Krebs & Timmermann, 2007; Stouffer et al., 2006; Yang et al., 2016; Yu et al., 2016). However, a recent study suggested that current models are not sensitive enough in their AMOC response (Liu et al., 2017), which implies that previous model projections of collapse probabilities are underestimated. The possibility of an AMOC collapse under global warming is a major concern due to its potentially dramatic impacts on oceanic circulation and global climate. The consequences of freshwater input near sites of deep water formation are a contemporary concern as the total freshwater storage of the North Atlantic increased by 19 000 km^3 between 1961 and 1995 (~0.02 Sv on average; Curry, 2005). This freshwater is transported to the Labrador Sea and creates salinity anomalies (Luo et al., 2016). It is therefore increasingly critical that we understand the impacts of climate change and freshwater release on convection in the Labrador Sea and its corresponding impact on AMOC intensity (Gregory et al., 2005). This is especially true if we are to identify the forcing(s) responsible for the ongoing AMOC weakening (Bakker et al., 2016; Thornalley et al., 2018).

High-resolution modeling (~10 km ocean, ~50 km atmosphere) suggests a robust relationship between a weakening AMOC and the decrease in the proportion of Labrador-derived water (Labrador Subarctic Slope Water : LSSW) entering the Northwest Atlantic shelf compared to Atlantic-derived water (Atlantic Temperate Slope Water : ATSW) under climate change (Saba et al., 2016). Interestingly, historical instrumental temperature data suggest a significant reorganisation of the Northwest Atlantic slope currents from the bottom water of the St. Lawrence Estuary (Gilbert et al., 2005). The significant bottom water warming (+1.7°C) during the twentieth-century was attributed to a decrease in the proportion (72 to 53%) of cool LSSW entering the Laurentian Channel (Gilbert et al., 2005). This warming was suggested to be unique over the last millennium (Thibodeau et al., 2010a) and the last ~6,000 years (Thibodeau et al., 2013). This major change in the regional oceanography has severe

environmental consequence, as the ATSW is characterized by lower dissolved oxygen content than the LSSW which, in conjunction with localized eutrophication, is thought to be responsible for the development of the permanent hypoxic zone in the St. Lawrence Estuary (Benoit et al., 2006; Gilbert et al., 2005; Lefort et al., 2012; Thibodeau et al., 2006; Thibodeau et al., 2010b). As detailed in figure 1, the recirculation gyre is considered to be controlled by the strength of the formation of deep water in the Labrador Sea and thus by the strength of the deep western boundary current (DWBC) (Zhang et al., 2007). A strong recirculation gyre keeps the Gulf Stream path well separated from the coast (Fig 1a) and allows for southern penetration of the LSSW. In episodes of weak convection characteristic of modern conditions (Rahmstorf et al., 2015), a larger proportion of the warm water from the Gulf Stream and ATSW is expected to be found in the Laurentian Channel bottom water (Fig 1b). It was further suggested that the westward transport of Labrador current water along the continental shelf edge to the south of the Grand Banks of Newfoundland could significantly contribute to temperature and salinity variability from the Gulf of St Lawrence to the Gulf of Maine (Petrie & Drinkwater, 1993). The contribution of AMOC and its component currents on regional temperature changes has led to the usage of ocean temperature as a surrogate for the AMOC intensities (e.g., the AMOC index; Rahmstorf et al., 2015), which has been later confirmed by high-resolution models (Saba et al., 2016). Moreover, a linear relationship was observed between the AMOC intensity and the AMOC index using the CMIP5 climate model ensemble (Caesar et al., 2018). Based on this relationship, it was estimated that AMOC intensity explains 89% of the variance in the temperature-based AMOC index with other factor having a minor influence on the observed temperature pattern (Caesar et al., 2018). Thus, the observed warming in the western North Atlantic and consequently in the Laurentian Channel could be linked to the weakened state of the AMOC (Caesar et al., 2018; Rahmstorf et al., 2015; Thornalley et al., 2018).

Here, we present two high-resolution records of oxygen isotope ($\delta^{18}O$) measurements of the benthic foraminifera *Globobulimina auriculata* covering the last century and the last 1,500 years respectively. We demonstrate how these records can be used to track sub-surface temperature of the western North Atlantic. We then tested this paleotemperature record against instrumental measurements, new model simulations, AMOC index and other AMOC-related proxies to link our record to the AMOC intensity. As such, we provide here one of the first robust high-resolution reconstructions of the strength of the AMOC over the last 1,500 years and highlight that the current AMOC is probably at its weakest state. While the uncertainties are larger when we investigate older periods, we further report statistically heavier $\delta^{18}O$ during

105 the Little Ice Age (LIA), which is interpreted as weaker AMOC conditions during that time.
106 Thus, our record is significant for the investigation of the potential mechanisms responsible for
107 the last century AMOC weakening.

108

109 **2. Methods**

110 We investigated the effects of an AMOC reduction on the western North Atlantic
111 subsurface temperature via freshwater perturbation experiments using two climate models: the
112 University of Victoria climate model (UVic v2.9) and the water isotope-enabled Community
113 Earth System Model (iCESM1.3). The UVic model is a climate model of intermediate
114 complexity including an ocean general circulation model at coarse resolution (3.6 × 1.8°, 19
115 vertical levels), a single-layer atmospheric energy-moisture balance model, a dynamic-
116 thermodynamic sea ice model, and biogeochemical components. The freshwater perturbation
117 experiment analyzed here has 0.05 Sv freshwater discharged into the North Atlantic between
118 45–65°N and 60–0°W for 100 years. Readers are referred to previous publications for a detailed
119 description of the experimental setup (Schmittner & Lund, 2015).

120 The water isotope-enabled Community Earth System Model version 1.3 (iCESM) is a
121 state-of-the-art fully coupled Earth system model with the capability to simulate the oxygen
122 isotopes in the hydrological cycle (Nusbaumer et al., 2017; Wong et al., 2017; Zhang et al.,
123 2017; Zhu et al., 2017a). The numerical experiments analyzed here are from a recent study
124 (Zhu et al., 2017b). The simulations were conducted with a horizontal resolution of 1.9 × 2.5°
125 (latitude × longitude) for the atmosphere and land, and a nominal 1° for the ocean and sea ice.
126 The ocean model consists of 60 uneven levels with an interval of ~10 m for the upper 200 m.
127 The preindustrial control simulation was run for 500 years, with forcing fixed at the values
128 from 1850 A.D., and water isotopes in the ocean initialized from the Goddard Institute for
129 Space Studies interpolated observational dataset (LeGrande & Schmidt, 2006). In the
130 freshwater perturbation experiment, 0.10 Sv of isotopically depleted fresh water was
131 discharged into the northern North Atlantic (50–70ºN) for 100 years. The $\delta^{18}O$ signature of the
132 freshwater forcing was set as –30 ‰ SMOW (Hillaire-Marcel & Causse, 1989). The simulation
133 of $\delta^{18}O$ in the model helps to test our interpretation of the benthic $\delta^{18}O$ records in the Laurentian
134 channel. The response of carbonate $\delta^{18}O$ (‰ PDB) to freshwater forcing is calculated in the
135 model with the simulated ocean temperature and $\delta^{18}O$ (‰ SMOW) of seawater, using the
136 paleotemperature equation of Shackleton (1974).

We then compiled $\delta^{18}O$ data (‰ VPDB) measured on the benthic foraminifera *Globobulimina auriculata* in two sediment cores (CR02-23 and MD99-2220; core details in S1-2) from the Laurentian Channel (Fig 1). The calcareous shells were picked under binocular and roasted at ~ 200ºC for about 2 hours in order to eliminate organic matter. Samples were analyzed with a Micromass Isoprime^{TM} isotope ratio mass spectrometer in dual inlet mode coupled to a MultiCarb^{TM} preparation system. The CO_2 was extracted at 90ºC by acidification with concentrated H_3PO_4. The analytical reproducibility determined by replicate measurements of internal standard carbonate material was routinely better than 0.05 ‰, which is equivalent to a precision of approximately 0.2°C..

3. Results and Discussion

3.1. Modelled effect of reduced AMOC on subsurface temperature

To test the link between AMOC strength and subsurface warming, the AMOC strength was reduced in two models (iCESM and UVic) (see detailed results in S3). Both models used here produced a large-scale subsurface warming in the northwest Atlantic at 45°N (Fig S1 and S2) with a maximum of 1–3°C around 50°W. The AMOC reduction obtained with the UVic model (~ 17 %) is consistent with the most recent estimate of weakening (Caesar et al., 2018; Rahmstorf et al., 2015; Thornalley et al., 2018). This subsurface warming of the western North Atlantic under weak AMOC conditions is expected from global gridded data set (Dima & Lohmann, 2010), theory (Petrie & Drinkwater, 1993; Zhang, 2008; Zhang et al., 2007), coarse (this study) as well as high-resolution and eddy-permitting models (Brickman et al., 2018; Caesar et al., 2018; Saba et al., 2016; Thornalley et al., 2018). Thus, the warming can be considered a robust fingerprint of the weakened AMOC. Moreover, the simulated water $\delta^{18}O$ is enriched by about 0.2–0.3‰ in the iCESM (Fig 2). This suggests a major increase in the proportion of $\delta^{18}O$-enriched ATSW in the subsurface water, indicating a change in western North Atlantic oceanography. This supports previous estimates based on temperature and dissolved oxygen changes (Gilbert et al., 2005; Thibodeau et al., 2010a).

3.2. Influence of temperature and water mass contribution on the $\delta^{18}O$ record

Due to the strong stratification in the Laurentian Channel, the temperature variation at our coring site reflects the temperature variation of the slope water entering the channel at

Cabot Strait (Gilbert et al., 2005). Thus, because of the high-sedimentation regime of this region, our cores provide a unique proxy of the slope water with a resolution of about 2 years per cm. It was demonstrated that isotopic signature of oxygen in *Globobulimina auriculata* tests is a good proxy of temperature change in the Laurentian Channel over the last century (Thibodeau, et al., 2010a). The warming instrumentally observed in the Laurentian Channel bottom water seems well captured by *Globobulimina auriculata* $\delta^{18}O$ in the high sedimentation box-core CR02-23 samples (Fig 3), as the $\delta^{18}O$ decreases from 1940 to 2000 by about 0.4 ‰ synchronously with the 2°C increase in temperature from the bottom water of the St. Lawrence Estuary. However, the $\delta^{18}O$ of benthic foraminifera also records the change in the proportion of water masses entering the Laurentian channel, as these water masses are characterized by different isotopic conditions. Using the isotopic signature of both water mass (ATSW = 0.5 ‰ and LSSW = -0.5 ‰), it was estimated that the proportion of these water masses is currently about 50-50 % (Thibodeau et al., 2010a). Based on dissolved oxygen and temperature, it was hypothesized that the proportion of ATSW entering the Laurentian channel was much lower in 1940 at about 30% (Gilbert et al., 2005), which imply an increase of $\delta^{18}O$ by about 0.2 ‰ between 1940 and 2000. We observed that the $\delta^{18}O$ of seawater exhibits an enrichment of 0.2 to 0.3 ‰ in the subsurface western North Atlantic in the freshwater perturbation experiment using iCESM (Fig 2), which is coherent with the magnitude of the increase in the proportion of ATSW entering the Laurentian Channel inferred from temperature and dissolved oxygen changes (Gilbert et al., 2005; Thibodeau et al., 2010a)). Considering a relationship of about -0.22 ‰/°C (Ravelo & Hillaire-Marcel, 2007), one would expect a decrease of -0.44 ‰ in the $\delta^{18}O$ of *Globobulimina auriculata* given the instrumentally-measured 2°C warming in the bottom water between 1940 and 2000. The increase in seawater $\delta^{18}O$ of at least 0.2 ‰ (from model and theory) combined to the expected decrease of about -0.44 ‰ due to higher temperature should translate into a decrease of -0.24 ‰ in the benthic foraminifera calcite. In our core, we observed a depletion of about 0.26 ‰ between the averaged pre-1940 values and the post-2000 values, which likely support the notion that part of the temperature effect was masked by the seawater $\delta^{18}O$ enrichment due to the change in water masses. While other potential factors could influence the $\delta^{18}O$ locally (mixing event, diffusion) they do not seem to be strong enough to mask the main signal driven by the AMOC as we demonstrated that 1) the AMOC influences the temperature of the slope water (Section 3.1 and references therein), 2) our site records these temperature variation (S4, Fig 3 and Gilbert et al., 2005) and 3) the $\delta^{18}O$ at our site records these temperature variation (section 3.2 and Thibodeau et al., 2010). We therefore suggest that the Laurentian Channel benthic $\delta^{18}O$ record is strongly influenced by

AMOC intensity via the advection of the western North Atlantic subsurface temperature and water mass dynamics.

3.3. Comparison with other AMOC-related proxies over the last century

An annually-resolved $\delta^{15}N$ record retrieved from soft corals over the Canadian shelf shows a high degree of similarity with both the $\delta^{18}O$ record and the instrumental record of temperature (Fig 3). This record was interpreted as an increase in the proportion of ATSW reaching the Canadian shelf, a unique event of the last 1800 years (Sherwood et al., 2011) and is consistent with the AMOC index (Caesar et al., 2018; Rahmstorf et al., 2015). The CR02-23 $\delta^{18}O$ record presented here is also in agreement with the AMOC index over the 1940-2000 period despite some leads and lags that can be attributed to either the different resolution and/or time integration of the respective proxies. The leads and lags could also be caused by the fact that the AMOC-index and our record integrate different signals; the AMOC-index estimates the difference in the temperature anomalies between the sub-polar gyre and the Northern Hemisphere while the $\delta^{18}O$ captures the temperature and water mass distribution of the slope water. Despite the potential caveats, the similarity between our $\delta^{18}O$ record, the temperature-based AMOC index, and instrumental data adds to the evidence linking the strength of the AMOC with the western North Atlantic subsurface temperature (Marcott et al., 2011; Petrie & Drinkwater, 1993; Saba et al., 2016), which implies that temperature can been used to diagnose the state of AMOC, as done previously (Caesar et al., 2018; Rahmstorf et al., 2015; Thornalley et al., 2018; Zhang, 2008). The $\delta^{18}O$ of benthic foraminifera in the Laurentian Channel can thus provide crucial information to reconstruct AMOC variability during the last century despite the fact that it incorporates both the temperature and the water mass signal.

The trend of $\delta^{18}O$ derived from the benthic foraminifera in long piston core MD99-2220 (hereafter MD) during the 20th century is unique in its magnitude for the last 1,500 years. While the current global warming trend could be invoked to explain this warming, we stress that neither of the parent water masses warmed significantly during the same period (Gilbert et al., 2005). Moreover, the absolute value of 1.5-2.0°C is much larger than the ~0.4°C attributed to the global trend (IPCC, 2013). Potential control from the North Atlantic Oscillation can also be discarded as no correlation with the temperature time series was observed (Gilbert et al., 2005). While still controversial, the reduction of the AMOC since the late 1930s and the drastic shift in North Atlantic overturning cell at the beginning of the 70's

234 was already identified using field data (Dima & Lohmann, 2010). The agreement between the
235 instrumental data, various climate archives, the two models, and the AMOC index lead us to
236 conclude that the weakening of the AMOC is a major factor causing the sub-surface warming
237 recorded in the sediment cores and corals compiled here. The evidence presented here thus
238 reinforces previous findings and provides complementary proxy-based evidence for the 20th
239 century AMOC slowdown.

240 While our record and modeling results strengthens the previous hypothesis regarding the
241 recent weakening of the AMOC and its consequences in the western North Atlantic, it also
242 highlights some discrepancies such as the 100-year difference in the beginning of the
243 weakening of the convection in the Labrador Sea (Thornalley et al., 2018) and the AMOC
244 (Caesar et al., 2018; Rahmstorf et al., 2015). Interestingly, our $\delta^{18}O$ record, interpreted as
245 being controlled by DWBC strength, mimics the AMOC index with a weakening starting
246 within the last century as opposed to the 19th century decline in the Labrador Sea convection
247 (Thornalley et al., 2018). While it is conceivable to invoke a potential lag between a reduced
248 convection in the Labrador Sea and its expression on surface waters, the pre-AD 1200
249 paleorecord does not seem to exhibit such lag, as the $\delta^{18}O$ matches the proxy for convection in
250 the Labrador Sea (Fig 4; see section 3.5). However, the amplitude of the recent weakening is
251 unique over this period and so caution should be exercised when directly using the paleorecord
252 to find the cause of this apparent mismatch. Moreover, the potential absence of decline in
253 Labrador Sea convection during the last part of 20th century (Böning et al., 2016) and the last
254 couple of decades (Yashayaev & Loder, 2016) also highlight the need to reconcile estimation
255 of convection in the Labrador Sea and the integrative AMOC proxies.

256 While it is possible to use our $\delta^{18}O$ proxy in longer reconstruction, it is not possible to
257 constrain $\delta^{18}O$ change solely to a change in the proportion of water masses as we did for the
258 last century since it is not known if the parent water masses temperature varied. As such,
259 potential temperature changes of the Gulf Stream (and ATSW) and Labrador Current (and
260 LSSW) should also be considered as a potential driver of $\delta^{18}O$ when analysing the pre-20th
261 century record.

262

263 *3.4. The 1600-1900 period*

264 While we observe a step-wise decrease in the AMOC starting in the late 15th century,
265 these variations are within the natural range of variability of our $\delta^{18}O$ record (Fig S6). However,

the 1600-1899 $\delta^{18}O$ values in core MD are significantly heavier compared to the pre-1600 record, suggesting a statistically weaker AMOC during the LIA. Alternative explanations for the low $\delta^{18}O$ during this period include a warming of either parent water mass, which would be counterintuitive for this time period (Keigwin, 1996). While the $\delta^{18}O$ of the Gulf Stream increased by about 0.1 ‰ between 1600 and 1900 (Saenger et al., 2011), it would account only for half of the increase observed in the MD core. Thus, a change in the proportion of the water masses entering the Laurentian Channel due to a weaker AMOC cannot be excluded at this point. At about AD 1850-1875, the sharp depletion in $\delta^{18}O$ is synchronous with the sudden decrease in DWBC intensity and Labrador Sea convection, which might be due to the beginning of the post-LIA ice cap melt and the consequent freshening of the Labrador Sea surface water (Koerner, 1977; Koerner & Fisher, 1990). While the MD core might record a weakened AMOC state during most of the LIA (1625-1850), its step-wise nature, rather than a continual weakening trend observed in the sortable silt record highlights a potential discrepancy between how the AMOC intensity is expressed in the $\delta^{18}O$ record and how it is translated in current velocity at 2,000 m depth, where the 48JPC and 56JPC cores were retrieved (Thornalley et al., 2018). Here, the potential interference from temperature and salinity changes in the parent water masses should be investigated in greater detail.

3.5. The pre-1600 period

The comparison of the MD core with the AMOC index highlights the absence of any trend within these two records throughout this period (Fig 4a). However, the MD record is characterized by more variability pre-AD 1500. This may be caused by the construction of the AMOC index based on multiple different proxies of SST in both the western North Atlantic and the subpolar North Atlantic, whereas the MD core records the subsurface signal at a single location, implying that the AMOC index integrates a much larger oceanic area and reduces the variability (Rahmstorf et al., 2015). This might alternatively be explained by subsurface temperature being slightly more sensitive to convection relative to the surface temperature. This is supported by the agreement pre-AD 1500 between the MD core and temperature and salinity reconstructions from the Labrador Sea (Fig 4b), which are considered effective proxies for Labrador Sea convection (Moffa-Sánchez et al., 2014). Thus, the $\delta^{18}O$ seems to record most of the natural variability of the Labrador Sea convection over that period.

4. Implications

Our record adds to the very few existing paleoreconstructions of AMOC for the last millennium and highlights the statistically weaker state of the AMOC during the 20th century. While our record substantiates previous finding, it also provides a unique high-resolution record of western North Atlantic sub-surface water evolution for the last millennium. The data provided here are thus important to disentangle the potential causes of the 20th century weakening, as they record sub-surface processes, which is different from the previously-published surface AMOC index (Caesar et al., 2018; Rahmstorf et al., 2015) and reconstruction of the DWBC (Thornalley et al., 2018). Moreover, the heavy $\delta^{18}O$ recorded during the LIA suggests a potential weakening of the AMOC during that period. These data could be used with temperature reconstructions of the Labrador current and Gulf Stream in order to further constrain the implication of the heavy $\delta^{18}O$ values during the LIA. By discussing the similarities and discrepancies between the records during the 20th century and LIA we provided new insights on the role of the Labrador Current in both weakening event but also the need to reconcile the different AMOC record with modern instrumental data. Our $\delta^{18}O$ record thus captures crucial information that will contribute to a better understanding of AMOC variability throughout the last 1,500 years and its drivers.

316 **5. Acknowledgments**

317 **Author contributions:** BT and CN designed the study, BT performed isotopic analyses
318 on CR02-23 and MD99-2220, AS performed the modeling with UVic2.9 and JZhu
319 performed the modeling with iCESM1.3. BT and CN wrote the manuscript with the
320 contribution of JZhu, AS, DN, CT, JZhang and ZL. We are thankful to the comments
321 provided by anonymous reviewers that helped improve the manuscript.
322

323 **Data and materials availability:** All data used in this paper are available in the online
324 material. The iCESM model codes are available through the National Center for
325 Atmospheric Research software development repository. The UVic model cores are
326 available at http://climate.uvic.ca/model/. Data for the UVic experiment are available
327 at http://www.clim-past.net/11/135/2015/cp-11-135-2015-supplement.zip.

328 **Figures and Tables**
329

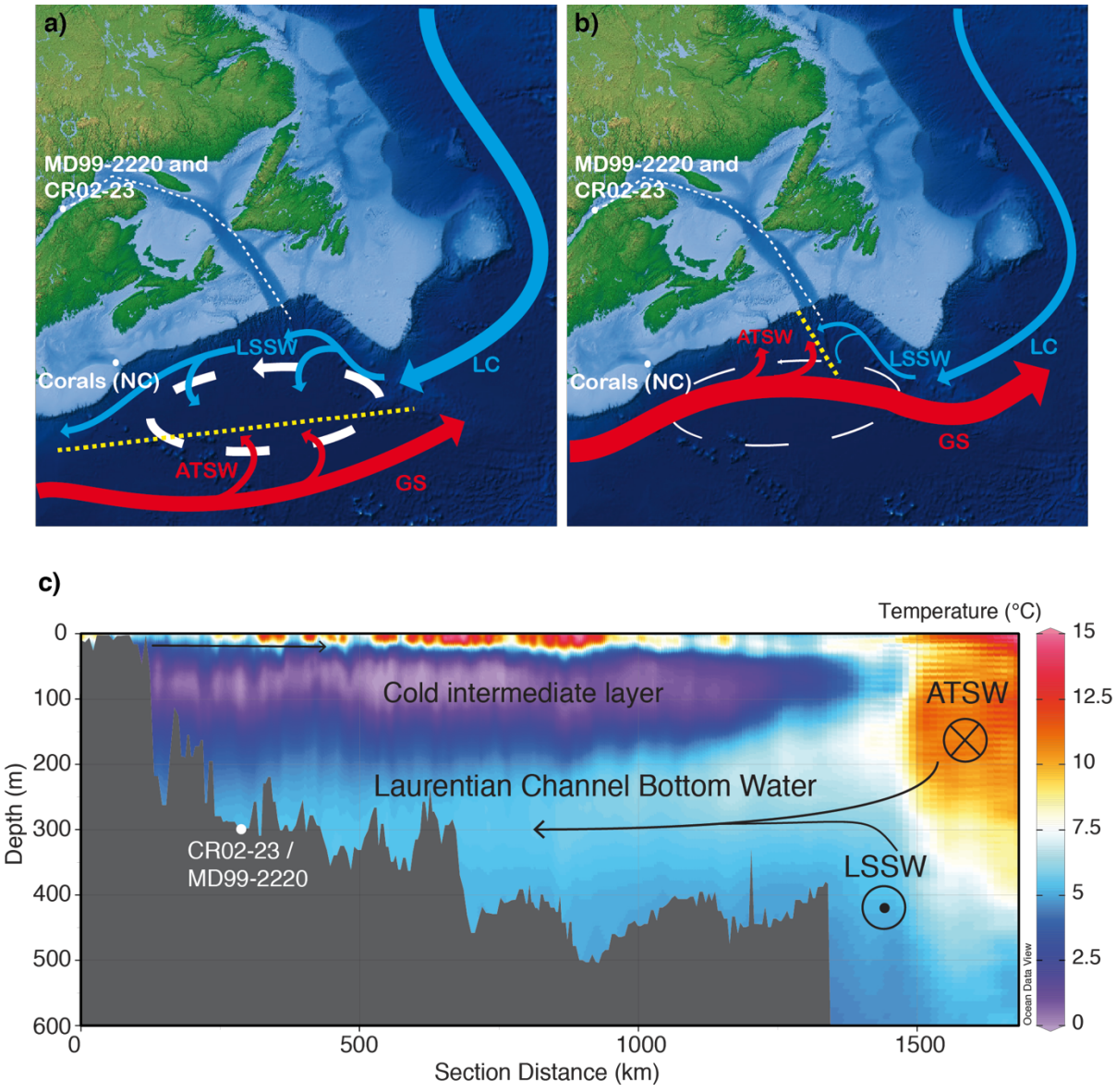

330
331

332 **Figure 1. Link between the strength of convection in the Labrador Sea, the**
333 **westward transport of Labrador current and the temperature across the Laurentian**
334 **Channel.** Schematic diagram of oceanic circulation near the entrance of the Laurentian
335 Channel in episodes of **a)** strong westward transport of Labrador Current (LC) and Labrador
336 Sea Slope Water (LSSW) with weaker influence of Atlantic Temperate Slope Water (ATSW)
337 derived from the Gulf Stream (GS) and **b)** weak westward transport of Labrador current and **c)**
338 the 2000-2010 averaged temperature (Levitus et al., 2013) profile along the Laurentian
339 Channel. The oceanography of the Northwest Atlantic is characterized by the interaction
340 between water masses formed in the Labrador Sea moving southward and the northward

341 flowing Gulf Stream. The exact location where these two water mass systems meet (yellow
342 dashed lines) is determined by the strength of the northern recirculation gyre (white arrows)
343 (Hogg et al., 1986). The width of the arrows represents the relative strength of the current.
344 White dots indicate the position of core MD99-2220 and CR02-23, which were cored close to
345 each other (respectively at; 48°38.32'N, 68°37.93'W; 320m and 48°42.01'N, 68°38.89'W;
346 345m). The position of corals raised from the Northeast Channel where a $\delta^{15}N$ time series was
347 recorded is also marked (42°00'N, 65°36'W, between 275 and 450 m) (Sherwood et al., 2011).
348 The temperature profile depicts the annually averaged position of the slope waters and how
349 they fill the bottom of the Laurentian Channel.
350

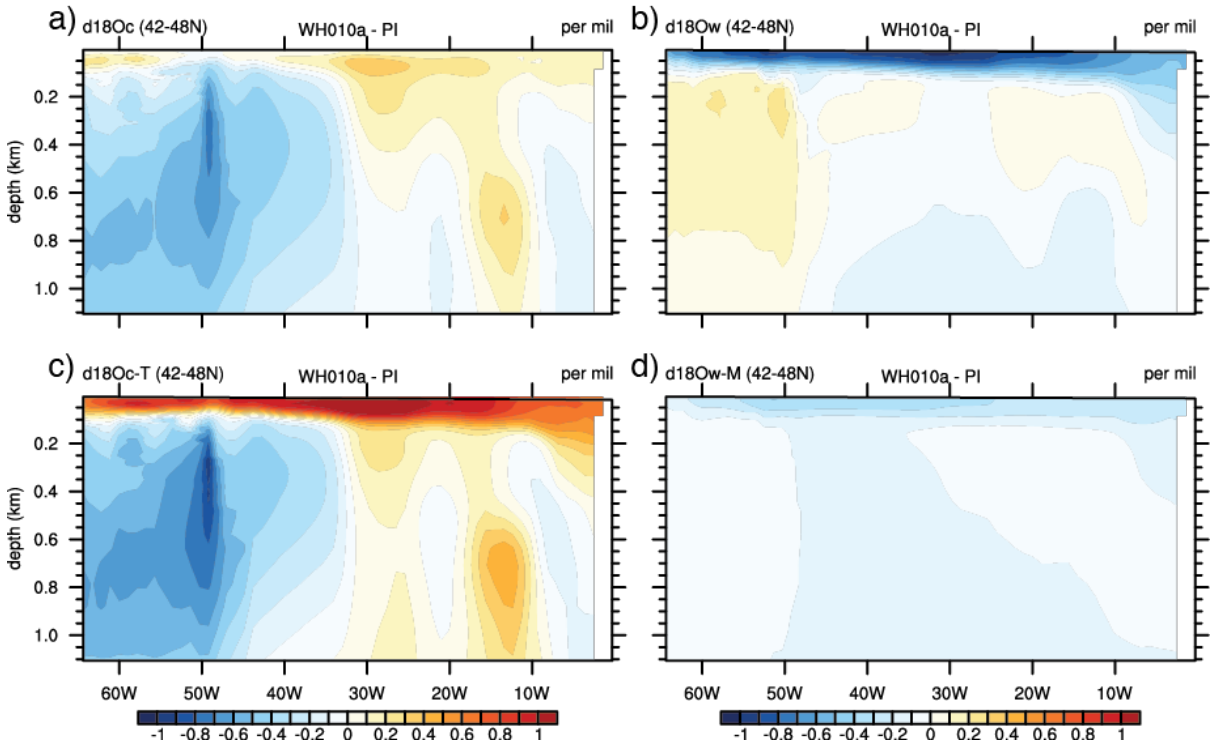

Figure 2. Attributing response of subsurface carbonate $\delta^{18}O$ to freshwater forcing in iCESM. a) Total changes in carbonate $\delta^{18}O$ (units: ‰ PDB) along 45°N in the North Atlantic calculated from modeled changes in seawater $\delta^{18}O$ (units: ‰ SMOW) and ocean temperature using the equation of Shackleton (1974), and contributions from **b)** changes in seawater $\delta^{18}O$ and **c)** ocean temperature. **d)** changes in seawater $\delta^{18}O$ (units: ‰ SMOW) coming from the direct meltwater effect, that is the direct depletion from the depleted freshwater forcing without changes in circulations.

361

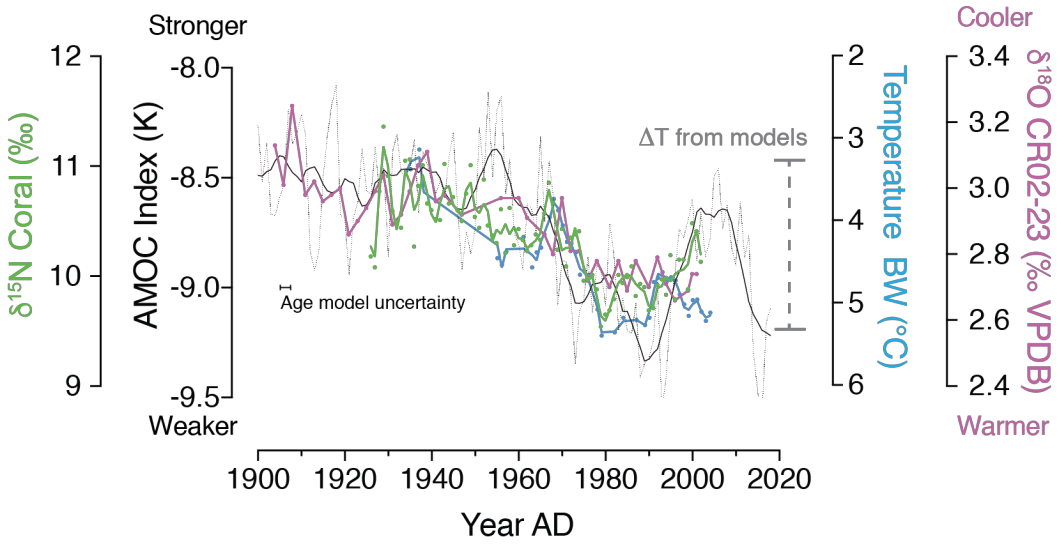

362

363 **Figure 3. Proxy validation using instrumental data and paleorecords.** The AMOC
364 index (Caesar et al., 2018) (black dotted line and smoothed black dashed line; 2nd order; 8
365 neighbors) and instrumental temperature record of Laurentian Channel bottom water (Gilbert
366 et al., 2005) (light blue dots and smoothed line; 2nd order, 2 neighbors) are plotted for the 1900-
367 2000 period along the annually resolved coral $\delta^{15}N$ record (Sherwood et al., 2011) (green dots
368 and smoothed line; 2nd order, 2 neighbors) that serves as a proxy of the strength of the northern
369 recirculation gyre and the modal state of the western North Atlantic circulation. The $\delta^{18}O$ of
370 benthic foraminifera from core CR02-23 (Thibodeau et al., 2010a) (pink) also shows the same
371 general pattern during that period. The average temperature increase (2°C) obtained at 400 m
372 deep in the western North Atlantic in our modelled AMOC-weakening experiments is indicated
373 by the gray bracket. An offset of 1.8 years was found between the lead-based age model and
374 the cesium peak and used to quantify the uncertainty, this offset is shown on the figure. The
375 analytical uncertainty of the lead-base age model (2σ) was found to be much smaller than the
376 offset displayed on the figure (S1).

377

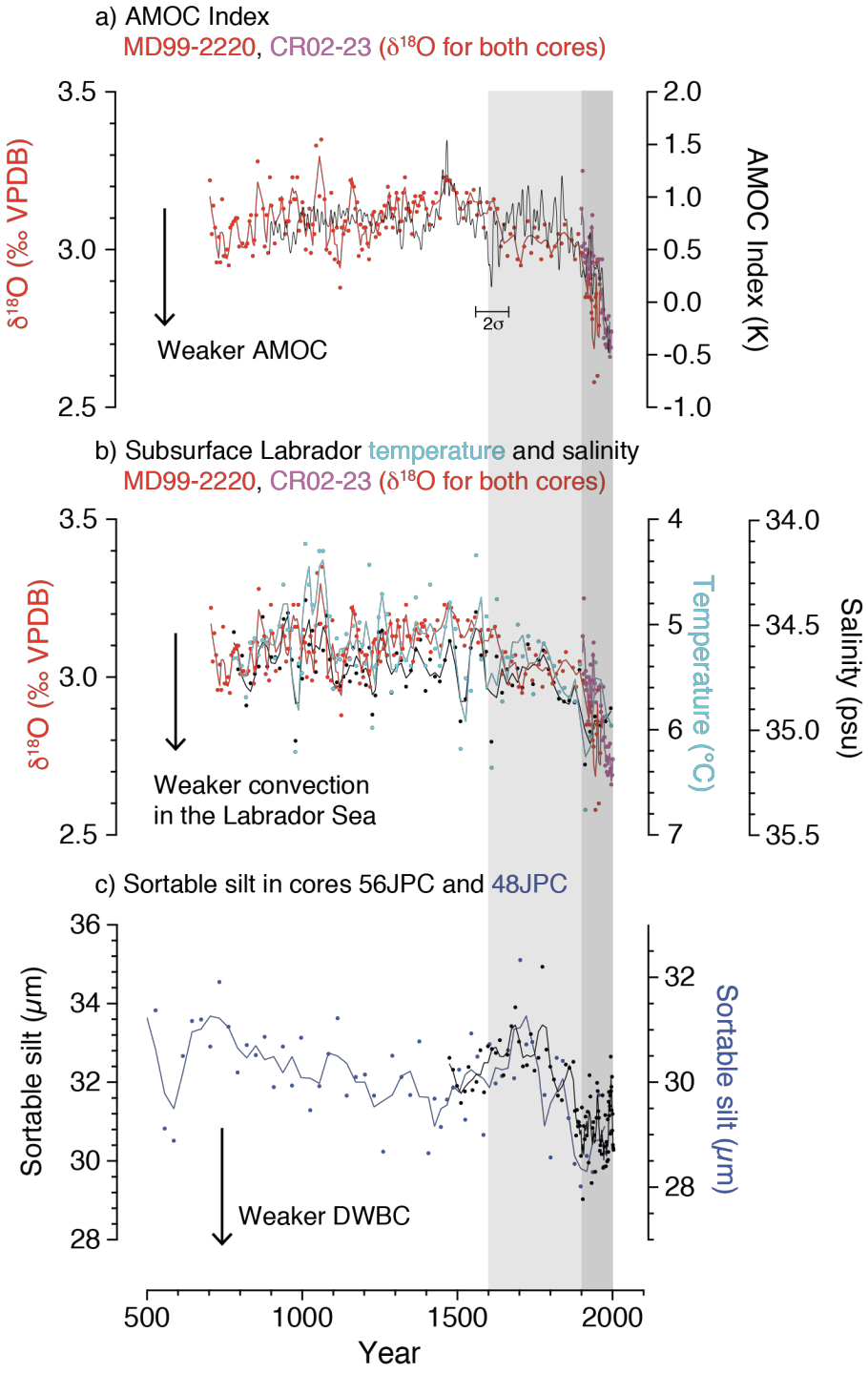

Figure 4. Comparison of North Atlantic climate archives covering the last millennium. The first panel **a)** comparison of composite (MD99-2220; red and CR02-23; pink) $\delta^{18}O$ *Globobulimina auriculata* record (smoothed lines; 2nd order, 2 neighbors) with the AMOC index (Rahmstorf et al., 2015) (black line). **b)** similarity of the composite (MD99-2220; red and CR02-23; pink) $\delta^{18}O$ record (smoothed lines; 2nd order, 2 neighbors) with reconstructed subsurface temperature (light blue dots) and salinity (black dots) of the Labrador Sea (Moffa-

386 Sánchez et al., 2014), which are indicative of convection in the Labrador Sea (smoothed lines;
387 2^{nd} order, 2 neighbors). **c)** sortable silt from two sediment cores retrieved off Cape Hatteras, a
388 proxy of the deep western boundary current (smoothed lines; 2^{nd} order, 2 neighbors)
389 (Thornalley et al., 2018). Grey bars highlight the LIA and the 20^{th} century. The 2σ value linked
390 to ^{14}C dating of core MD99-2220 (St-Onge et al., 2003) is shown on the graph.

391

392

393 Bakker, P., Schmittner, A., Lenaerts, J. T. M., Abe-Ouchi, A., Bi, D., van den Broeke, M. R.,
394 et al. (2016). Fate of the Atlantic Meridional Overturning Circulation: Strong decline
395 under continued warming and Greenland melting. *Geophysical Research Letters*,
396 *43*(23), 12,252-12,260. https://doi.org/10.1002/2016GL070457
397 Benoit, P., Gratton, Y., & Mucci, A. (2006). Modeling of dissolved oxygen levels in the
398 bottom waters of the Lower St. Lawrence Estuary: Coupling of benthic and pelagic
399 processes. *Marine Chemistry*, *102*(1–2), 13–32.
400 https://doi.org/10.1016/j.marchem.2005.09.015
401 Bohm, E., Lippold, J., Gutjahr, M., Frank, M., Blaser, P., Antz, B., et al. (2015). Strong and
402 deep Atlantic meridional overturning circulation during the last glacial cycle. *Nature*,
403 *517*(7532), 73–76. Retrieved from http://dx.doi.org/10.1038/nature14059
404 Böning, C. W., Behrens, E., Biastoch, A., Getzlaff, K., & Bamber, J. L. (2016). Emerging
405 impact of Greenland meltwater on deepwater formation in the North Atlantic Ocean.
406 *Nature Geosci*, *9*(7), 523–527. Retrieved from http://dx.doi.org/10.1038/ngeo2740
407 Brickman, D., Hebert, D., & Wang, Z. (2018). Mechanism for the recent ocean warming
408 events on the Scotian Shelf of eastern Canada. *Continental Shelf Research*, *156*, 11–22.
409 https://doi.org/10.1016/j.csr.2018.01.001
410 Caesar, L., Rahmstorf, S., Robinson, A., Feulner, G., & Saba, V. (2018). Observed
411 fingerprint of a weakening Atlantic Ocean overturning circulation. *Nature*, *556*(7700),
412 191–196. https://doi.org/10.1038/s41586-018-0006-5
413 Curry, R. (2005). Dilution of the Northern North Atlantic Ocean in Recent Decades. *Science*,
414 *308*(5729), 1772–1774. https://doi.org/10.1126/science.1109477
415 Delworth, T. L., Clark, P. U., Holland, M., Johns, W. E., Kuhlbrodt, T., Lynch-Stieglitz, J., et
416 al. (2008). The Potential for Abrupt Change in the Atlantic Meridional Overturning
417 Circulation. *Abrupt Climate Change*, 117–162. Retrieved from
418 http://citeseerx.ist.psu.edu/viewdoc/download?doi=10.1.1.184.709&rep=rep1&type=pdf
419 %5Cnhttp://downloads.climatescience.gov/sap/sap3-4/sap3-4-final-report-ch4.pdf
420 Dima, M., & Lohmann, G. (2010). Evidence for Two Distinct Modes of Large-Scale Ocean
421 Circulation Changes over the Last Century. *Journal of Climate*, *23*(1), 5–16.
422 https://doi.org/10.1175/2009JCLI2867.1
423 Gilbert, D., Sundby, B., Gobeil, C., Mucci, A., & Tremblay, G. H. (2005). A seventy-two-
424 year record of diminishing deep-water oxygen in the St. Lawrence estuary: The
425 northwest Atlantic connection. *Limnology and Oceanography*, *50*(5), 1654–1666.
426 https://doi.org/10.4319/lo.2005.50.5.1654
427 Gregory, J. M., Dixon, K. W., Stouffer, R. J., Weaver, A. J., Driesschaert, E., Eby, M., et al.
428 (2005). A model intercomparison of changes in the Atlantic thermohaline circulation in
429 response to increasing atmospheric CO2 concentration. *Geophysical Research Letters*,
430 *32*(12), 1–5. https://doi.org/10.1029/2005GL023209
431 Hillaire-Marcel, C., & Causse, C. (1989). The late pleistocene Laurentide glacier: Th U
432 dating of its major fluctuations and δ18O range of the ice. *Quaternary Research*, *32*(2),
433 125–138. https://doi.org/10.1016/0033-5894(89)90070-7
434 Hogg, N. G., Pickart, R. S., Hendry, R. M., & Smethie, W. J. (1986). The northern
435 recirculation gyre of the gulf Stream. *Deep Sea Research Part A, Oceanographic*
436 *Research Papers*, *33*(9), 1139–1165. https://doi.org/10.1016/0198-0149(86)90017-8
437 IPCC. (2013). *Climate Change 2013: The Physical Science Basis. Summary for*
438 *Policymakers*. *IPCC*. Retrieved from
439 http://medcontent.metapress.com/index/A65RM03P4874243N.pdf
440 Jungclaus, J. H., Haak, H., Esch, M., Roeckner, E., & Marotzke, J. (2006). Will Greenland
441 melting halt the thermohaline circulation? *Geophysical Research Letters*, *33*(17).
442 https://doi.org/10.1029/2006GL026815

443 Keigwin, L. D. (1996). The Little Ice Age and Medieval Warm Period in the Sargasso Sea.
444 *Science*, *274*(5292), 1503–1508. https://doi.org/10.1126/science.274.5292.1503
445 Koerner, R. M. (1977). Devon Island Ice Cap: Core Stratigraphy and Paleoclimate. *Science*,
446 *196*(4285), 15–18. https://doi.org/10.1126/science.196.4285.15
447 Koerner, R. M., & Fisher, D. A. (1990). A record of Holocene summer climate from a
448 Canadian high-Arctic ice core. *Nature*, *343*(6259), 630–631.
449 https://doi.org/10.1038/343630a0
450 Krebs, U., & Timmermann, A. (2007). Fast advective recovery of the Atlantic meridional
451 overturning circulation after a Heinrich event. *Paleoceanography*, *22*(1), 1–9.
452 https://doi.org/10.1029/2005PA001259
453 Lefort, S., Gratton, Y., Mucci, a., Dadou, I., & Gilbert, D. (2012). Hypoxia in the Lower St.
454 Lawrence Estuary: How physics controls spatial patterns. *Journal of Geophysical*
455 *Research*, *117*(C7), C07018. https://doi.org/10.1029/2011JC007751
456 LeGrande, A. N., & Schmidt, G. A. (2006). Global gridded data set of the oxygen isotopic
457 composition in seawater. *Geophysical Research Letters*, *33*(12).
458 https://doi.org/10.1029/2006GL026011
459 Levitus, S., Antonov, J. I., Baranova, O. K., Boyer, T. P., Coleman, C. L., Garcia, H. E., et al.
460 (2013). The World Ocean Database. *Data Science Journal*, *12*(0), WDS229-WDS234.
461 https://doi.org/10.2481/dsj.WDS-041
462 Liu, W., Xie, S.-P., Liu, Z., & Zhu, J. (2017). Overlooked possibility of a collapsed Atlantic
463 Meridional Overturning Circulation in warming climate. *Science Advances*, *3*(1).
464 Retrieved from http://advances.sciencemag.org/content/3/1/e1601666.abstract
465 Luo, H., Castelao, R. M., Rennermalm, A. K., Tedesco, M., Bracco, A., Yager, P. L., &
466 Mote, T. L. (2016). Oceanic transport of surface meltwater from the southern Greenland
467 ice sheet. *Nature Geoscience*, *9*(7), 528–532. https://doi.org/10.1038/ngeo2708
468 Marcott, S. A., Clark, P. U., Padman, L., Klinkhammer, G. P., Springer, S. R., Liu, Z., et al.
469 (2011). Ice-shelf collapse from subsurface warming as a trigger for Heinrich events.
470 *Proceedings of the National Academy of Sciences of the United States of America*,
471 *108*(33), 13415–13419. https://doi.org/10.1073/pnas.1104772108
472 Moffa-Sánchez, P., Hall, I. R., Barker, S., Thornalley, D. J. R., & Yashayaev, I. (2014).
473 Surface changes in the eastern Labrador Sea around the onset of the Little Ice Age.
474 *Paleoceanography*, *29*(3), 160–175. https://doi.org/10.1002/2013PA002523
475 Nusbaumer, J., Wong, T. E., Bardeen, C., & Noone, D. (2017). Evaluating hydrological
476 processes in the Community Atmosphere Model Version 5 (CAM5) using stable isotope
477 ratios of water. *Journal of Advances in Modeling Earth Systems*, *9*(2), 949–977.
478 https://doi.org/10.1002/2016MS000839
479 Petrie, B., & Drinkwater, K. (1993). Temperature and salinity variability on the Scotian Shelf
480 and in the Gulf of Maine 1945–1990. *Journal of Geophysical Research*, *98*(C11),
481 20079. https://doi.org/10.1029/93JC02191
482 Rahmstorf, S., Box, J. E., Feulner, G., Mann, M. E., Robinson, A., Rutherford, S., &
483 Schaffernicht, E. J. (2015). Exceptional twentieth-century slowdown in Atlantic Ocean
484 overturning circulation. *Nature Climate Change*, *5*(5), 475–480.
485 https://doi.org/10.1038/nclimate2554
486 Ravelo, A. C., & Hillaire-Marcel, C. (2007). The Use of Oxygen and Carbon Isotopes of
487 Foraminifera in Paleoceanography. In *Developments in Marine Geology* (Vol. 1, pp.
488 735–764). https://doi.org/10.1016/S1572-5480(07)01023-8
489 Saba, V. S., Griffies, S. M., Anderson, W. G., Winton, M., Alexander, M. A., Delworth, T.
490 L., et al. (2016). Enhanced warming of the Northwest Atlantic Ocean under climate
491 change. *Journal of Geophysical Research: Oceans*, *121*(1), 118–132.
492 https://doi.org/10.1002/2015JC011346

493 Saenger, C., Came, R. E., Oppo, D. W., Keigwin, L. D., & Cohen, A. L. (2011). Regional
494 climate variability in the western subtropical North Atlantic during the past two
495 millennia. *Paleoceanography*, *26*(2). https://doi.org/10.1029/2010PA002038
496 Schmittner, A., & Lund, D. C. (2015). Early deglacial Atlantic overturning decline and its
497 role in atmospheric CO2 rise inferred from carbon isotopes (d13C). *Climate of the Past*,
498 *11*(2), 135–152. https://doi.org/10.5194/cp-11-135-2015
499 Shackleton, N. J. (1974). Attainment of isotopic equilibrium between ocean water and the
500 benthonic foraminifera geuns *Uvigerina*: Isotopic changes in the ocean during the last
501 glacial. *Colloques Internationaux Du C.N.R.S.*, *219*, 203–210.
502 Sherwood, O. A., Lehmann, M. F., Schubert, C. J., Scott, D. B., & McCarthy, M. D. (2011).
503 Nutrient regime shift in the western North Atlantic indicated by compound-specific
504 δ15N of deep-sea gorgonian corals. *Proceedings of the National Academy of Sciences of*
505 *the United States of America*, *108*(3), 1011–5. https://doi.org/10.1073/pnas.1004904108
506 St-Onge, G., Stoner, J. S., & Hillaire-Marcel, C. (2003). Holocene paleomagnetic records
507 from the St. Lawrence Estuary, eastern Canada: centennial- to millennial-scale
508 geomagnetic modulation of cosmogenic isotopes. *Earth and Planetary Science Letters*,
509 *209*(1–2), 113–130. https://doi.org/10.1016/S0012-821X(03)00079-7
510 Stouffer, R. J., Yin, J., Gregory, J. M., Dixon, K. W., Spelman, M. J., Hurlin, W., et al.
511 (2006). Investigating the Causes of the Response of the Thermohaline Circulation to
512 Past and Future Climate Changes. *Journal of Climate*, *19*(8), 1365–1387.
513 https://doi.org/10.1175/JCLI3689.1
514 Thibodeau, B., de Vernal, A., & Mucci, A. (2006). Recent eutrophication and consequent
515 hypoxia in the bottom waters of the Lower St. Lawrence Estuary: Micropaleontological
516 and geochemical evidence. *Marine Geology*, *231*(1–4), 37–50.
517 https://doi.org/10.1016/j.margeo.2006.05.010
518 Thibodeau, B., Lehmann, M. F., Kowarzyk, J., Mucci, A., Gélinas, Y., Gilbert, D., et al.
519 (2010). Benthic nutrient fluxes along the Laurentian Channel: Impacts on the N budget
520 of the St. Lawrence marine system. *Estuarine, Coastal and Shelf Science*, *90*(4), 195–
521 205. https://doi.org/10.1016/j.ecss.2010.08.015
522 Thibodeau, B., de Vernal, A., Hillaire-Marcel, C., & Mucci, A. (2010). Twentieth century
523 warming in deep waters of the Gulf of St. Lawrence: A unique feature of the last
524 millennium. *Geophysical Research Letters*, *37*(17).
525 https://doi.org/10.1029/2010GL044771
526 Thibodeau, B., de Vernal, A., & Limoges, A. (2013). Low oxygen events in the Laurentian
527 Channel during the Holocene. *Marine Geology*, *346*, 183–191.
528 https://doi.org/10.1016/j.margeo.2013.08.004
529 Thornalley, D. J. R., Oppo, D. W., Ortega, P., Robson, J. I., Brierley, C. M., Davis, R., et al.
530 (2018). Anomalously weak Labrador Sea convection and Atlantic overturning during the
531 past 150 years. *Nature*, *556*(7700), 227–230. https://doi.org/10.1038/s41586-018-0007-4
532 Wong, T. E., Nusbaumer, J., & Noone, D. C. (2017). Evaluation of modeled land-atmosphere
533 exchanges with a comprehensive water isotope fractionation scheme in version 4 of the
534 Community Land Model. *Journal of Advances in Modeling Earth Systems*, *9*(2), 978–
535 1001. https://doi.org/10.1002/2016MS000842
536 Yang, Q., Dixon, T. H., Myers, P. G., Bonin, J., Chambers, D., & Van Den Broeke, M. R.
537 (2016). Recent increases in Arctic freshwater flux affects Labrador Sea convection and
538 Atlantic overturning circulation. *Nature Communications*, *7*.
539 https://doi.org/10.1038/ncomms10525
540 Yashayaev, I., & Loder, J. W. (2016). Recurrent replenishment of Labrador Sea Water and
541 associtated decadal-scale variability. *Journal Geophysical Research: Oceans*, *121*,
542 8095–8114. https://doi.org/10.1002/2016JC012046.Received

Yu, L., Gao, Y., & Otterå, O. H. (2016). The sensitivity of the Atlantic meridional overturning circulation to enhanced freshwater discharge along the entire, eastern and western coast of Greenland. *Climate Dynamics*, *46*(5–6), 1351–1369. https://doi.org/10.1007/s00382-015-2651-9

Zhang, J., Liu, Z., Brady, E. C., Oppo, D. W., Clark, P. U., Jahn, A., et al. (2017). Asynchronous warming and δ 18 O evolution of deep Atlantic water masses during the last deglaciation. *Proceedings of the National Academy of Sciences*, *114*(42), 11075–11080. https://doi.org/10.1073/pnas.1704512114

Zhang, R. (2008). Coherent surface-subsurface fingerprint of the Atlantic meridional overturning circulation. *Geophysical Research Letters*, *35*(20), L20705. https://doi.org/10.1029/2008GL035463

Zhang, R., Vallis, G. K., Fluid, G., Oceanic, N., & Program, O. S. (2007). The Role of Bottom Vortex Stretching on the Path of the North Atlantic Western Boundary Current and on the Northern Recirculation Gyre. *Journal of Physical Oceanography*, *37*(8), 2053–2080. https://doi.org/10.1175/JPO3102.1

Zhu, J., Liu, Z., Brady, E. C., Otto-Bliesner, B. L., Marcott, S. A., Zhang, J., et al. (2017). Investigating the Direct Meltwater Effect in Terrestrial Oxygen-Isotope Paleoclimate Records Using an Isotope-Enabled Earth System Model. *Geophysical Research Letters*, *44*, 12501–12510. https://doi.org/10.1002/2017GL076253

Zhu, J., Liu, Z., Brady, E., Otto-Bliesner, B., Zhang, J., Noone, D., et al. (2017). Reduced ENSO variability at the LGM revealed by an isotope-enabled Earth system model. *Geophysical Research Letters*, *44*(13), 6984–6992. https://doi.org/10.1002/2017GL073406

568 **Supporting information for:**

569 # Last century warming over the Canadian Atlantic shelves linked to weak
570 # Atlantic Meridional Overturning Circulation

571

572

573 **Authors**

574 B. Thibodeau[1,2]†*, C. Not[1,2]†, J. Zhu[3], A. Schmittner[4], D. Noone[4], C. Tabor[5], J. Zhang[6], Z.
575 Liu[7]

576

577 **Affiliations**

578 [1]Department of Earth Sciences, The University of Hong Kong, Hong Kong SAR

579 [2]The Swire Institute of Marine Science, The University of Hong Kong, Hong Kong SAR

580 [3]Department of Earth and Environmental Sciences, University of Michigan, United-States of
581 America

582 [4]College of Earth, Ocean, and Atmospheric Sciences, Oregon State University, United-States
583 of America

584 [5]Center for Integrative Geosciences, University of Connecticut, United-States of America

585 [6]CCS-2 and CNLS, Los Alamos National Laboratory, Los Alamos, New Mexico, United-
586 States of America

587 [7]Atmospheric Science Program, Department of Geography, The Ohio State University,
588 United-States of America

589

590 *Correspondence to: bthib@hku.hk

591 † Equal contribution

592

593

594

595 **Content**

596 Text S1 to S5

597 Figures S1 to S5

598

599 **Additional file**

600 Full dataset (excel file)

601

602 **Introduction**

603 This file includes additional details about modeling results, sediment cores chronology and
604 uncertainty of the proxy used as well as statistic on the results.
605

606 **1. Chronostratigraphy of climate archives**

607 The chronostratigraphy of core MD99-2220 was originally established by St-Onges et
608 al. (2003) based on twenty benthic mollusk shells analyzed from MD99-2220 and neighbor
609 core MD99-2221. Correlation with a box core retrieved from the same site indicated that the
610 top 14 cm of core MD99-2220 was missing. The age model of the upper part of core MD99-
611 2220 was established using a box-core retrieved from the same vicinity. The cross-correlation
612 between MD99-2220 and AH00-2220 was performed based on geochemical data (St-Onge et
613 al., 2003; Thibodeau et al., 2006; Thibodeau et al., 2010a). The chronostratigraphy of box core
614 CR02-23 (taken at the same site) was validated using ^{210}Pb (Thibodeau et al., 2006). Here we
615 present an updated age model for both cores using a constant-rate supply ^{210}Pb model that
616 calculates variable sedimentation rate for each sample, which is particularly suitable for last-
617 century cores where sedimentation rate often changes due to anthropogenic activities (Ghaleb,
618 2009) (Fig S4). We calculated the analytical uncertainty using the constant initial concentration
619 model, which respectively yielded error of ± 0.16 and 0.14 year per cm (± 2σ) for core AH00-
620 2220 and CR02-23. An offset of 1.8 years was found between the lead-based age model and
621 the cesium-137 peak. (Fig S3). Due to the loss of the top 14 cm of core MD99-2220, we will
622 not use this core for high-resolution reconstruction of the last century and rather focus on core
623 CR02-23. While the benthic foraminifera δ^{18}O values are similar for both cores and decrease
624 toward the younger part of the core, there is an offset of about 40 years between the appearance
625 of the lowest value in the two cores (Fig S4). This offset could be due to sediment
626 disturbance/compression in the upper part of the piston core.

627 The chronostratigraphy of gorgonian coral was done using band-counting validated by
628 radiocarbon measurement (Sherwood et al., 2011). The subsurface Labrador Sea temperature
629 and salinity record comes from sediment core RAPiD-35-25B (Moffa-Sánchez et al., 2014).
630 We used the original chronology, which is based on ^{210}Pb dating of the upper part of the core
631 and seven ^{14}C dates in the older part of the core (Moffa-Sánchez et al., 2014).

632

633 **2. Uncertainties of different proxies**

634 Measurement of δ^{18}O in core MD99-2220 and CR02-23 was performed with an
635 analytical precision better than ±0.05 ‰, which is equivalent to a precision of about 0.15-
636 0.20°C in temperature. Instrumental measurements of Laurentian Channel bottom water
637 temperature were carried out with a precision of ±0.01°C (Gilbert et al., 2005). Nitrogen

638 isotopes of coral were measured with an analytical precision better than ±0.20‰ (Sherwood et
639 al., 2011). Subsurface salinity and temperature reconstruction of the Labrador Sea have an
640 uncertainty of ±0.8 psu and ±0.8°C (Moffa-Sánchez et al., 2014). Analytical precision for
641 sortable silt was estimated at 1% (±0.3 μm), while replicates-based precision was estimated at
642 ±0.8 μm (Thornalley et al., 2018).

643

644 **3. Modeling results**

645 In response to the freshwater forcing (0.05 Sv in the UVic and 0.10 Sv in the iCESM),
646 the upper-ocean seawater becomes fresher and lighter, increasing stratification and inhibiting
647 deep convection in the North Atlantic (Fig S1). As a result, the AMOC strength, indicated by
648 the maximum transport in the North Atlantic, decreases by 17% and 28% in 100 years in UVic
649 and iCESM, respectively. The warming is a consequence of reduced northward transport in the
650 Gulf Stream, which requires a decrease in zonal density (temperature) gradients via thermal
651 wind balance. The models achieve this by warming west and cooling east of ~40°W. Modeling
652 results suggest that the reorganization of gyre circulations is a direct consequence of AMOC
653 weakening (Saba et al., 2016; Thornalley et al., 2018). The reduced northward heat transport
654 associated with the AMOC decreases the SST in the northern North Atlantic significantly and
655 produces a local high-pressure anomaly (Stouffer et al., 2006). The high-pressure anomaly acts
656 to weaken the westerlies in the mid-latitude North Atlantic and the gyre circulations. A budget
657 analysis of the subsurface temperature changes in iCESM was conducted. The analysis
658 suggests that the net subsurface warming is primarily caused by the reduced zonal component
659 of the Gulf Stream, as the reduced meridional flow acts to cool the subsurface water (Fig S2).
660 It is important to note that we only applied freshwater forcing at the ocean surface and kept all
661 other boundary conditions and forcings constant, as the parent water masses did not warm
662 during the last century (Gilbert et al., 2005). Therefore, the subsurface temperature increase is
663 solely due to a change in the circulation. In summary, both models suggest a warming of
664 intermediate water in the Northwestern Atlantic of 1.5–2.5°C (Fig S1) under a weakening of
665 the AMOC by 17–28%.

666 The water-isotope capability of iCESM can also help to further validate that our
667 sedimentary $\delta^{18}O$ records actually represent changes in temperature by investigating the
668 contribution of changes in $\delta^{18}O$ of seawater. The simulated water $\delta^{18}O$ enrichment of about
669 0.2–0.3‰ suggests a major increase in the proportion of saltier, $\delta^{18}O$-enriched water from the

Gulf Stream and ATSW (Fig 2). The heavier modelled $\delta^{18}O$ also discards potential effect related to the injection of freshwater in the system. This seawater $\delta^{18}O$ enrichment could influence our benthic $\delta^{18}O$ record in the opposite way than warming, which depletes the $\delta^{18}O$ recorded in carbonate. Therefore, the amplitude of our temperature reconstruction should be considered as a conservative estimation. While a sensitivity experiment conducted with iCESM (iPOP2-Trace) suggests that the $\delta^{18}O$ of carbonate at the MD99-2220 coring location might be heavier because of change in pCO_2 (Zhang et al., 2017), the effect is also opposite to the signal observed in our record.

4. Oxygen isotopes as a record for temperature

Oxygen isotopes in carbonate marine organisms vary with the temperature of calcification and the $\delta^{18}O$ value of the water mass in which they calcify (Shackleton, 1974). This counteracting effect has been previously investigated in Laurentian channel sediment cores by comparing high-resolution benthic foraminifera $\delta^{18}O$ records to instrumental temperature and salinity data (Thibodeau et al., 2010a). It was demonstrated that $\delta^{18}O$ in benthic foraminifera underestimated the actual temperature increase (i.e., creating lighter $\delta^{18}O$) because of the increased proportion of Atlantic Intermediate Slope Water (characterized by high $\delta^{18}O$) in the Laurentian Channel. Thus, our $\delta^{18}O$ records from the St. Lawrence should be considered as a conservative tool to reconstruct the Laurentian Channel bottom water temperature, as the full temperature increase is not expressed. This signal was also observed in the model results (Fig 2), which further support our hypothesis. The relatively rapid residence time (about 7 years) and the isolation of the Laurentian channel bottom water from overlying freshwater make it resilient to other potential local processes affecting $\delta^{18}O$ and thus representative of the western North Atlantic slope waters entering the channel, irrespective of the timescale (Gilbert et al., 2005). This is further illustrated by the absence of statistically different changes in temperature and salinity along the same potential density from Cabot Strait though the St. Lawrence Estuary between 1970 and 1990, highlighting the potential for these cores to reflect the condition of the water entering the channel (Gilbert et al., 2005). Because the temperature of the bottom is directly controlled by the proportion of Atlantic Intermediate Slope Water entering the Laurentian channel, the $\delta^{18}O$ in benthic foraminifera can also be considered a tracer of changes in the regional oceanography.

5. Statistical analysis

We investigated the similarity of the 20th century Laurentian channel bottom water instrumental temperature, $\delta^{15}N$ of corals and the AMOC index (Caesar et al., 2018) and how well $\delta^{18}O$ of core CR02-23 recorded these trends (Fig 3) using a spearman correlation (non-parametric). We did not detrend the data, as we are mostly interested in how well the $\delta^{18}O$ of core CR02-23 captures the general trend and we wanted to minimize the influence of potential lead and lag due to sample resolution, bioturbation smoothing, and variable sedimentation rates. Results suggest a high degree of similarity between CR02-23 $\delta^{18}O$ and instrumental temperature ($r = -0.76$, $p < 0.005$), CR02-23 $\delta^{18}O$ and coral $\delta^{15}N$ ($r = 0.79$, $p < 0.005$), and CR02-23 $\delta^{18}O$ and AMOC index ($r = 0.70$, $p < 0.0001$). We also observed a high correlation between the AMOC index and instrumental temperature ($r = -0.55$, $p < 0.005$), and the coral $\delta^{15}N$ ($r = 0.62$, $p < 0.005$). The coral $\delta^{15}N$ is also similar to the instrumental temperature ($r = -0.77$, $p < 0.005$).

The 20th century values in core MD are significantly different when comparing them to both the complete record (~700–1960), the pre-1600, and the 1600-1899 period ($p < 0.005$ for both Kruskal-Wallis and one-way ANOVA). Using the same tests, we found that the 1600-1899 period is not significantly different from the complete record, but it is significantly different from the pre-1600 record ($p < 0.05$ for both Kruskal-Wallis and one-way ANOVA). The means and the 95% confidence interval for each period can be seen in Fig S5.

722 Supplementary Figures

723 Figure 1. Modelled impact of a weakening of the AMOC on the temperature in the western
724 North Atlantic.

725 Figure 2. Budget analysis of the subsurface warming.

726 Figure 3. Updated age models for core piston core MD99-2220 and its box core AH00-2220
727 and box core CR02-23.

728 Figure 4. $\delta^{18}O$ from core MD99-2220 (red) and CR02-23 (pink) and $\delta^{15}N$ from Sherwood's
729 corals.

730 Figure 5. Means and confidence intervals (95%) of the different time periods in core MD99-
731 2220

732

733

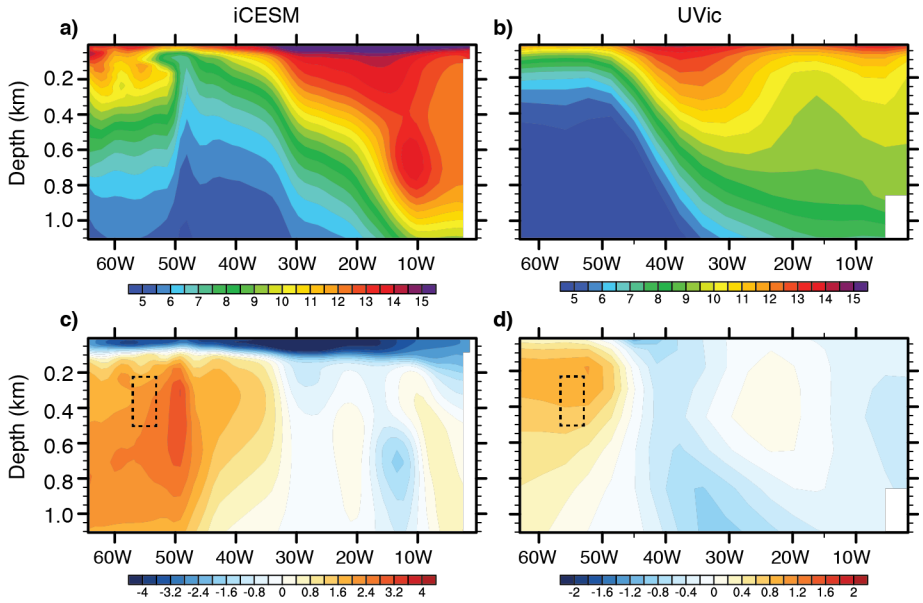

Figure S1. Modelled impact of a weakening of the AMOC on the temperature in the western North Atlantic. In the bottom panel we illustrate the modeled ocean temperature changes over the Northwest Atlantic after 100 years of freshwater forcing in the iCESM and UVic model. Depth-longitude section of ocean temperature in the upper 1,000 m of the western North Atlantic at 45°N in the preindustrial control simulation (**a,b**) and the changes after 100-year water hosing (**c,d**). We can observe the warming of the intermediate water of 2–2.5°C and 1–1.5°C next to the Laurentian channel entrance (dashed boxes) in the iCESM and UVic model, respectively. Note that the magnitude of the freshwater forcing is 0.10 Sv in the iCESM and 0.05 Sv in the UVic model.

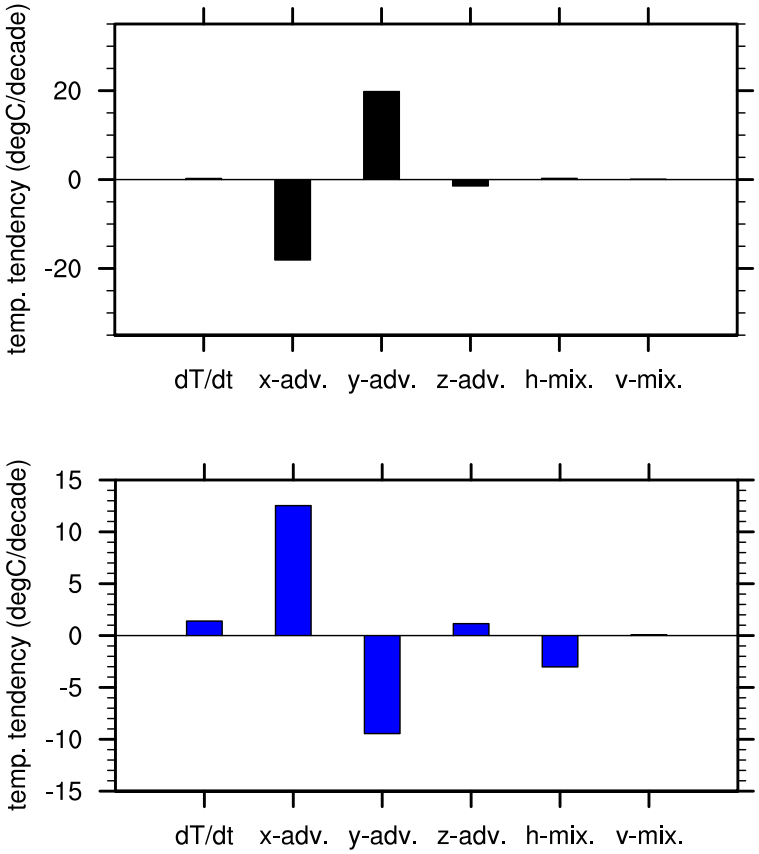

Figure S2. Budget analysis of the subsurface warming. Terms in the temperature equation of the northwestern North Atlantic subsurface ocean (44–46°N, 300–320°E, 400m) in the preindustrial control simulation in iCESM (left; units: °C decade^{-1}). From left to right are: the temperature tendency, the zonal advection, the meridional advection, the vertical advection, the horizontal mixing and vertical mixing. Bottom panel shows the changes averaged between year 91 and 100 in the freshwater perturbation experiments. We note that the subsurface warming is dominantly caused by change in the zonal component of gyre circulations, which is coherent with a reorganization of the subsurface current suggested in Fig 1.

780

781

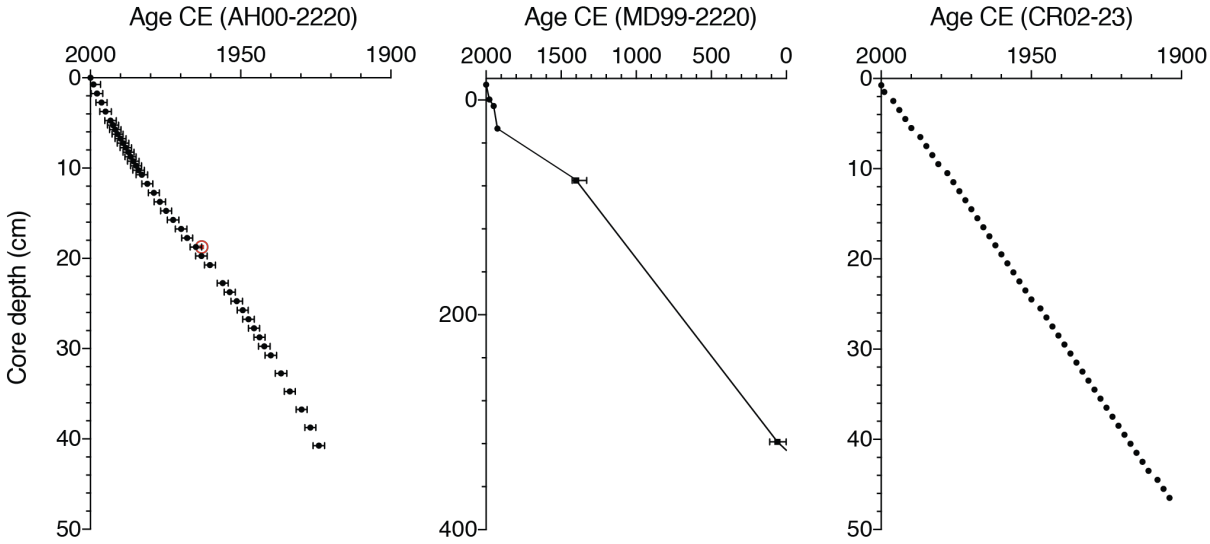

782

783

784 **Figure S3. Updated age models for core piston core MD99-2220 and its box core AH00-**
785 **2220 and box core CR02-23.** We updated the ^{210}Pb-derived age model for box cores AH00-
786 2220 and CR02-23 by using the constant rate supply model (Ghaleb, 2009; Sanchez-Cabeza &
787 Ruiz-Fernández, 2012), which estimate the age of each layer independently (i.e., the
788 sedimentation rate can vary in this model). Previous models have used a constant initial
789 concentration model, which implies a constant sedimentation rate. The precision (±1.8 years)
790 of the ^{210}Pb-derived age model for box core AH00-2220 was determined by comparing the
791 ^{210}Pb-derived age to the highest concentration of ^{137}Cs (1964.8), which is attributed to the peak
792 (red dot) of nuclear testing in 1963 (Left panel). The middle panel shows the composite age
793 model for piston core MD99-2220, which lost its top 14 cm in the coring process. The right
794 panel represents the ^{210}Pb-derived age model for box core CR02-23. Detailed data and
795 calculation for the age models are available in the online data.

796

797

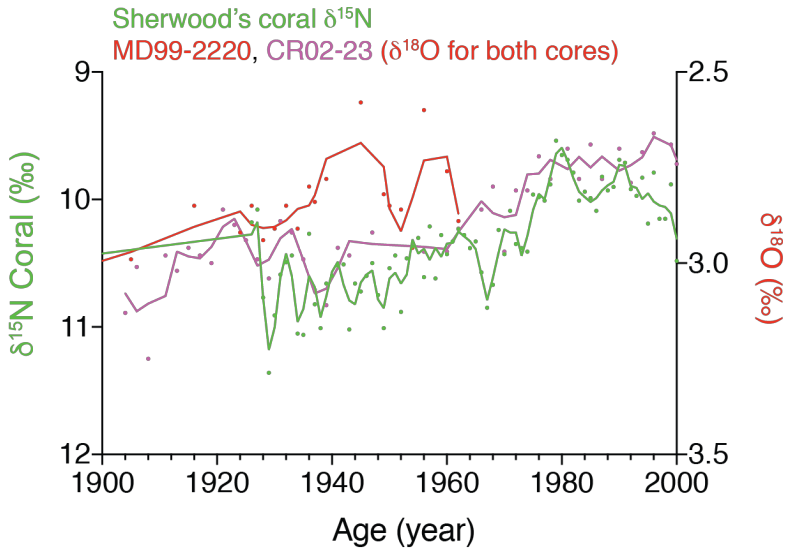

Figure S4. $\delta^{18}O$ from core MD99-2220 (red) and CR02-23 (pink) and $\delta^{15}N$ from Sherwood's corals. The $\delta^{18}O$ at 1900 is 3‰ for MD99-2220 and 3.10‰ for CR02-23. The lowest value is 2.6‰ for MD and 2.66‰ for CR. Thus, the amplitude of the change is similar. There is a clear offset between the dating of the lowest value, which happen much faster in core MD. Since we know the top of the core was lost during the piston coring of MD, we rather not used this part of the core and focus our high-resolution analysis on the box core CR that is well dated with ^{210}Pb

809

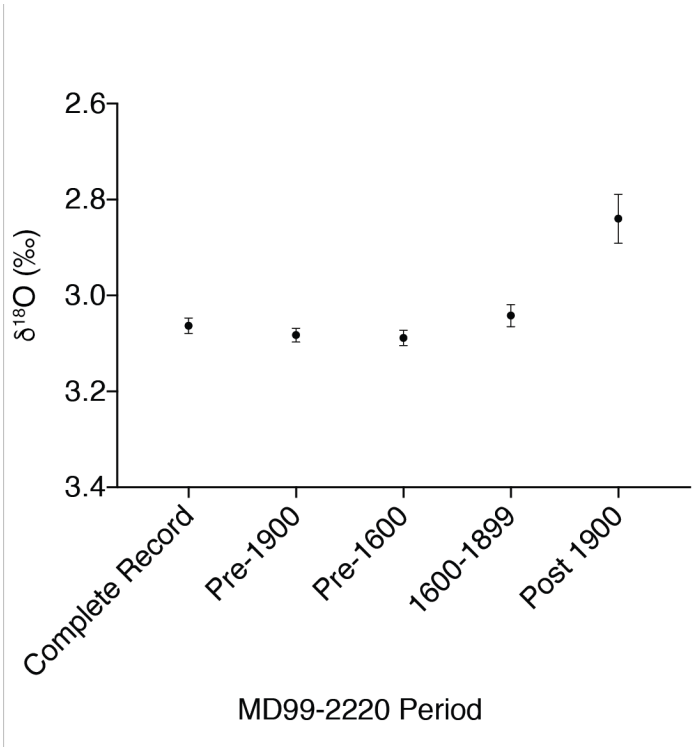

810

811 **Figure S5. Means and confidence intervals (95%) of the different time periods in core**
812 **MD99-2220.** The post-1900 period is significantly different than any other period while the
813 1600-1899 period is significantly different than the pre-1600 period.

814
815